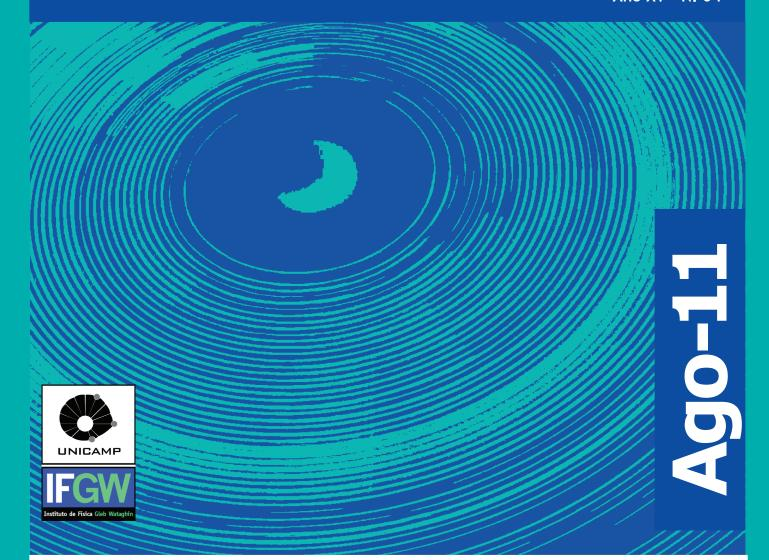
Abstracta

Ano XV - N. 04



Trabalhos Publicados

Julho 2011 à Agosto 2011

P104-11 à P150 -11

Material Editorial

Capítulo de Livro

Trabalhos Publicados

[P104-11] "A novel method to extract dark matter parameters from neutrino telescope data"

Esmaili, A. and Farzan, Y.

Recently it has been shown that when the Dark Matter (DM) particles captured in the Sun directly annihilate into neutrino pairs, the oscillatory terms in the oscillation probability do not average to zero and can lead to a seasonal variation as the distance between the Sun and Earth changes in time. In this paper, we explore this feature as a novel method to extract information on the properties of dark matter. We show that by studying the variation of the flux over a few months, it would in principle be possible to derive the DM mass as well as new information on the flavor structure of the DM annihilation modes. In addition to analytic analysis, we present the results of our numerical calculations that take into account scattering and regeneration of neutrinos traversing the Sun

Journal of Cosmology and Astroparticle Physics [4]. 007.2011.

[P105-11] "Active to Sterile Neutrino Mixing Limits from Neutral-Current Interactions in MINOS"

Adamson, P., Auty, D. J., Ayres, D. S., Backhouse, C., Barr, G., Bishai, M., Blake, A., Bock, G. J., Boehnlein, D. J., Bogert, D., Cavanaugh, S., Cherdack, D., et all

Results are reported from a search for active to sterile neutrino oscillations in the MINOS long-baseline experiment, based on the observation of neutral-current neutrino interactions, from an exposure to the NuMI neutrino beam of 7.07 x 10(20) protons on target. A total of 802 neutral-current event candidates is observed in the Far Detector, compared to an expected number of 754 +/- 28(stat) +/- 37(syst) for oscillations among three active flavors. The fraction f(s) of disappearing nu(mu) that may transition to nu(s) is found to be less than 22% at the 90% C.L

Physical Review Letters 107[1]. 011802. 2011.

[P106-11] "Anisotropy and chemical composition of ultrahigh energy cosmic rays using arrival directions measured by the Pierre Auger Observatory"

Abreu, P., Aglietta, M., Ahn, E. J., Albuquerque, J. F. M., Allard, D., Allekotte, I., Allen, J., Allison, P., Castilo, J. A., Alvarez-Muniz, J., Ambrosio, M., Aminaei, A., Anchordoqui, L., et all

The Pierre Auger Collaboration has reported. evidence for anisotropy in the distribution of arrival directions of the cosmic rays with energies $E > E(th) = 5.5 \times 10(19)$ eV. These show a correlation with the distribution of nearby extragalactic objects, including an apparent excess around the direction of Centaurus A. If the particles responsible for these excesses at E > E(th) are heavy nuclei with charge Z, the proton component of the sources should lead to excesses in the same regions at energies E/Z. We here report the lack of anisotropies in these directions at energies above E(th)/Z (for illustrative values of Z = 6, 13, 26). If the anisotropies above E(th) are due to nuclei with charge Z, and under reasonable assumptions about the acceleration process, these observations imply stringent constraints on the allowed proton fraction at the lower energies

Journal of Cosmology and Astroparticle Physics [6]. 022.2011.

[P107-11] "Circular polarization in a non-magnetic resonant tunneling device"

dos Santos, L. F., Gobato, Y. G., Teodoro, M. D., Lopez-Richard, V., Marques, G. E., Brasil, M. J. S. P., Orlita, M., Kunc, J., Maude, D. K., Henini, M., and Airey, R. J.

We have investigated the polarization-resolved photoluminescence (PL) in an asymmetric n-type GaAs/AlAs/GaAlAs resonant tunneling diode under magnetic field parallel to the tunnel current. The quantum well (QW) PL presents strong circular polarization (values up to -70% at 19 T). The optical emission from GaAs contact layers shows evidence of highly spin-polarized two-dimensional electron and hole gases which affects the spin polarization of carriers in the QW. However, the circular polarization degree in the QW also depends on various other parameters, including the g-factors of the different layers, the density of carriers along the structure, and the Zeeman and Rashba effects

Nanoscale Research Letters 6. 101. 2011.

[108-11] "Comparison of the sensitivity of extraordinary transmittance peaks with the surrounding media for hole and slit arrays"

Menezes, J. W., Avila, L. F., Braga, E. S., and Cescato, L.

In this paper we compare the sensitivity of the Extraordinary Transmittance (ET) peak position with the surrounding media for two types of metallic structures: arrays of holes and arrays of slits recorded in Au films. Both types of array were fabricated using Interference Lithography (IL) with a period of 700 nm and an Au thickness of 150 nm. The transmission spectra measurements were performed at normal incidence using a spectrophotometer. The results show that an array of slits presents a higher sensitivity for the surrounding media than the array of holes. Theoretical TE and TM simulations of the transmission spectra for the slit arrays agree very well with the experimental results, confirming the better sensitivity of the slit arrays

Applied Physics A-Materials Science & Processing 103[3], 631-634. 2011.

[P109-11] "Conservation law for distributed entanglement of formation and quantum discord"

Fanchini, F. F., Cornelio, M. F., de Oliveira, M. C., and Caldeira, A. O.

We present a direct relation, based upon a monogamic principle, between entanglement of formation (EOF) and quantum discord (QD), showing how they are distributed in an arbitrary tripartite pure system. By extending it to a paradigmatic situation of a bipartite system coupled to an environment, we demonstrate that the EOF and the QD obey conservation relation. By means of this relation we show that in the deterministic quantum computer with one pure qubit the protocol has the ability to rearrange the EOF and the QD, which implies that quantum computation can be understood on a different basis as a coherent dynamics where quantum correlations are distributed between the qubits of the computer. Furthermore, for a tripartite mixed state we show that the balance between distributed EOF and QD results in a stronger version of the strong subadditivity of entropy

Physical Review A 84[1]. 012313. 2011.

[P110-11] "Constraining nonstandard neutrino interactions with electrons"

Forero, D. V. and Guzzo, M. M.

We update the phenomenological constraints of the nonstandard neutrino interactions (NSNI) with electrons including in the analysis, for the first time, data from LAMPF, Krasnoyarsk, and the latest Texono observations. We assume that NSNI modify the cross section of elastic scattering of (anti) neutrinos off electrons, using reactor and accelerator data, and the cross section of the electron-positron annihilation, using the four LEP experiments, in particular, new data from DELPHI. We find more restrictive allowed regions for the NSNI parameters: 0.11 < epsilon(eR)(ee) < 0.05 and -0.02 < epsilon(eL)(ee) < 0.050.09 (90% C.L.). We also recalculate the parameters of tauonic flavor obtaining -0.35 < epsilon(eR)(tau tau) < 0.50 and -0.51 < epsilon(eL)(tau tau) < 0.34 (90% C.L.). Although more severe than the limits already present in the literature, our results indicate that NSNI are allowed by the present data as a subleading effect, and the standard electroweak model continues consistent with the experimental panorama at 90% C.L. Further improvement on this picture will deserve a lot of engagement of upcoming experiments

Physical Review D 84[1]. 013002. 2011.

[P111-11] "Destroying a near-extremal Kerr-Newman black hole"

Saa, A. and Santarelli, R.

We revisit here a previous argument due to Wald showing the impossibility of turning an extremal Kerr-Newman black hole into a naked singularity by plunging test particles across the black hole event horizon. We extend Wald's analysis to the case of near-extremal black holes and show that it is indeed possible to destroy their event horizon, giving rise to naked singularities, by pushing test particles toward the black hole as, in fact, it has been demonstrated explicitly by several recent works. Our analysis allows us to go a step further and to determine the optimal values, in the sense of keeping to a minimum the backreaction effects, of the test particle electrical charge and angular momentum necessary to destroy a given near-extremal Kerr-Newman black hole. We describe briefly a possible realistic scenario for the creation of a Kerr naked singularity from some recently discovered candidates to be rapidly rotating black holes in radio galaxies

Physical Review D 84[2]. 027501.2011.

[P112-11] "Diffusion Limited Aggregation: Algorithm optimization revisited"

Braga, F. L. and Ribeiro, M. S.

The Diffusion Limited Aggregation (DLA) model developed by Witten and Sander in 1978 is useful in modeling a large class of growth phenomena with local dependence. Besides its simplicity this aggregation model has a complex behavior that can be observed at the patterns generated. We propose on this work a brief review of some important proprieties of this model and present an algorithm to simulate a DLA aggregates that simpler and efficient compared to others found in the literature. (C) 2011 Elsevier By. All rights reserved

Computer Physics Communications 182[8], 1602-1605. 2011.

[P113-11] "Effect of O(2)(+), H(2)(+) + O(2)(+), and N(2)(+) + O(2)(+) ion-beam irradiation on the field emission properties of carbon nanotubes"

Acuna, J. J. S., Escobar, M., Goyanes, S. N., Candal, R. J., Zanatta, A. R., and Alvarez, F.

The effect of O(2)(+), H(2)(+) + O(2)(+), and N(2)(+) + O(2)(+)ion-beam irradiation of carbon nanotubes (CNTs) films on the chemical and electronic properties of the material is reported. The CNTs were grown by the chemical vapor deposition technique (CVD) on silicon TiN coated substrates previously decorated with Ni particles. The Ni decoration and TiN coating were successively deposited by ion-beam assisted deposition (IBAD) and afterwards the nanotubes were grown. The whole deposition procedure was performed in situ as well as the study of the effect of ionbeam irradiation on the CNTs by x-ray photoelectron spectroscopy (XPS). Raman scattering, field-effect emission gun scanning electron microscopy (FEG-SEM), and field emission (FE) measurements were performed ex situ. The experimental data show that: (a) the presence of either H(2)(+) or N(2)(+) ons in the irradiation beam determines the oxygen concentration remaining in the samples as well as the studied structural characteristics; (b) due to the experimental conditions used in the study, no morphological changes have been observed after irradiation of the CNTs; (c) the FE experiments indicate that the electron emission from the CNTs follows the Fowler-Nordheim model, and it is dependent on the oxygen concentration remaining in the samples; and (d) in association with FE results, the XPS data suggest that the formation of terminal quinone groups decreases the CNTs work function of the material. (C) 2011 American Institute of Physics. [doi: 10.1063/1.3593269]

Journal of Applied Physics 109[11]. 114317. 2011.

[P114-11] "Effect of oxygen adsorption on magnetic properties of graphite"

Boukhvalov, D. W., Moehlecke, S., da Silva, R. R., and Kopelevich, Y.

Both experimental and theoretical studies of the magnetic properties of micrographite and nanographite indicate a crucial role of the partial oxidation of graphitic zigzag edges in ferromagnetism. In contrast to total and partial hydrogenation, the oxidation of half of the carbon atoms on the graphite edges transforms the antiferromagnetic exchange interaction between graphite planes and over graphite ribbons to the ferromagnetic interaction. The stability of the ferromagnetism is discussed

Physical Review B 83[23]. 233408. 2011.

[P115-11] "Effect of synthesis conditions on the microstructure of TEOS derived silica hydrogels synthesized by the alcohol-free sol-gel route"

Perullini, M., Jobbagy, M., Bilmes, S. A., Torriani, I. L., and Candal, R.

Silica matrices synthesized from a pre-hydrolysis step in ethanol followed by alcohol removal at low pressure distillation, and condensation in water, are suitable for encapsulation of biomolecules and microorganisms and building bioactive materials with optimized optical properties. Here we analyze the microstructure of these hydrogels from the dependence of I(q) data acquired from SAXS experiments over a wide range of silica concentration and pH employed in the condensation step. From the resulting data it is shown that there is a clear correlation between the microscopic parameters-cluster fractal dimension (D), elementary particle radius (a) and cluster

gyration radius (R)-with the attenuation of visible light when the condensation step proceeds at pH < 6. At higher pHs, there is a steep dependence of the cluster density (similar to R (D-3)) with the condensation pH, and non-monotonous changes of attenuance are less than 20%, revealing the complexity of the system. These results, which were obtained for a wide pH and silica concentration range, reinforce the idea that the behavior of gels determined in a restricted interval of synthesis variables cannot be extrapolated, and comparison of gelation times is not enough for predicting their properties

Journal of Sol-Gel Science and Technology 59[1], 174-180. 2011.

[P116-11] "Electromagnetically induced blazed grating at low light levels"

Carvalho, S. A. and de Araujo, L. E. E.

We propose a scheme for inducing a blazed transmission grating in a four-level, N-type atomic medium under electromagnetically induced transparency (EIT). The blazed grating relies on the giant Kerr nonlinearity that the atomic medium exhibits under EIT. The grating is created using an intensity mask in one of the driving optical fields and only weak fields with intensities below saturation level are involved. Diffraction efficiencies of a resonant probe beam close to 100% are predicted

Physical Review A 83[5]. 053825. 2011.

[P117-11] "Energy dissipation via coupling with a finite chaotic environment"

Marchiori, M. A. and de Aguiar, M. A. M.

We study the flow of energy between a harmonic oscillator (HO) and an external environment consisting of N two-degrees-offreedom nonlinear oscillators, ranging from integrable to chaotic according to a control parameter. The coupling between the HO and the environment is bilinear in the coordinates and scales with system size as 1/root N. We study the conditions for energy dissipation and thermalization as a function of N and of the dynamical regime of the nonlinear oscillators. The study is classical and based on a single realization of the dynamics, as opposed to ensemble averages over many realizations. We find that dissipation occurs in the chaotic regime for fairly small values of N, leading to the thermalization of the HO and the environment in a Boltzmann distribution of energies for a well-defined temperature. We develop a simple analytical treatment, based on the linear response theory, that justifies the coupling scaling and reproduces the numerical simulations when the environment is in the chaotic regime

Physical Review e 83[6]. 061112. 2011.

[P118-11] "Enhanced magneto-optical oscillations from twodimensional hole-gases in the presence of Mn ions"

Gazoto, A. L., Brasil, M. J. S. P., Iikawa, F., Brum, J. A., Ribeiro, E., Danilov, Y. A., Vikhrova, O. V., and Zvonkov, B. N.

We investigated the effects of nearby Mn ions on the optical properties of two-dimensional hole-gases confined in InGaAs/GaAs quantum wells. We observed energy oscillations on both the averaged emission and the spin-splitting energies, whereas the first one presents maxima at all integer filling factors, and the second one, solely at odd-filling factors. The strength of the oscillations clearly increases with the Mn concentration. Furthermore, considering the relatively low-mobility of our structures, the oscillations are surprisingly strong and robust, persisting up to relatively high temperatures and excitation

intensities. (C) 2011 American Institute of Physics. [doi:10.1063/1.3601477]

Applied Physics Letters 98[25]. 251901. 2011.

[P119-11] "Entanglement Irreversibility from Quantum Discord and Quantum Deficit"

Cornelio, M. F., de Oliveira, M. C., and Fanchini, F. F.

We relate the problem of irreversibility of entanglement with the recently defined measures of quantum correlation-quantum discord and one-way quantum deficit. We show that the entanglement of formation is always strictly larger than the coherent information and the entanglement cost is also larger in most cases. We prove irreversibility of entanglement under local operations and classical communication for a family of entangled states. This family is a generalization of the maximally correlated states for which we also give an analytic expression for the distillable entanglement, the relative entropy of entanglement, the distillable secret key, and the quantum discord

Physical Review Letters 107[1]. 020502. 2011.

[P120-11] "Experimental studies of di-jet survival and surface emission bias in Au plus Au collisions via angular correlations with respect to back-to-back leading hadrons"

Agakishiev, H., Aggarwal, M. M., Ahammed, Z., Alakhverdyants, A. V., Alekseev, I., Alford, J., Anderson, B. D., Anson, C. D., Arkhipkin, D., Averichev, G. S., Balewski, J., et all

We report first results from an analysis based on a new multihadron correlation technique, exploring jet-medium interactions and di-jet surface emission bias at the BNL Relativistic Heavy Ion Collider (RHIC). Pairs of back-to-back high-transversemomentum hadrons are used for triggers to study associated hadron distributions. In contrast with two-and three-particle correlations with a single trigger with similar kinematic selections, the associated hadron distribution of both trigger sides reveals no modification in either relative pseudorapidity Delta eta or relative azimuthal angle Delta phi from d + Au to central Au + Au collisions. We determine associated hadron yields and spectra as well as production rates for such correlated back-to-back triggers to gain additional insights on medium properties

Physical Review C 83[6]. 061901. 2011.

[P121-11] "First-order reversal curves acquired by a high precision ac induction magnetometer"

Beron, F., Soares, G., and Pirota, K. R.

We present a setup allowing to characterize the local irreversible behavior of soft magnetic samples. It is achieved by modifying a conventional ac induction magnetometer in order to measure first-order reversal curves (FORCs), a magnetostatic characterization technique. The required modifications were performed on a home-made setup allowing high precision measurement, with sensibility less than 0.005 Oe for the applied field and 10(-6) emu for the magnetization. The main crucial point for the FORCs accuracy is the constancy of the applied field sweep rate, because of the magnetic viscosity. Therefore, instead of the common way to work at constant frequency, each FORC is acquired at a slightly different frequency, in order to keep the field variation constant in time. The obtained results exhibit the consequences of magnetic viscosity, thus opening up the path of studying this phenomenon for soft magnetic materials.

(C) 2011 American Institute of Physics. [doi:10.1063/1.3600796]

Review of Scientific Instruments 82[6]. 063904. 2011.

[P122-11] "First Direct Observation of Muon Antineutrino Disappearance"

Adamson, P., Andreopoulos, C., Auty, D. J., Ayres, D. S., Backhouse, C., Barr, G., Bishai, M., Blake, A., Bock, G. J., Boehnlein, D. J., Bogert, D., Cavanaugh, S., et all

This Letter reports the first direct observation of muon antineutrino disappearance. The MINOS experiment has taken data with an accelerator beam optimized for (nu) over bar (mu) production, accumulating an exposure of 1.71 x 10(20) protons on target. In the Far Detector, 97 charged current (nu) over bar (mu) events are observed. The no-oscillation hypothesis predicts 156 events and is excluded at 6.3 sigma. The best fit to oscillation yields vertical bar Delta(m) over bar (2)vertical bar = [3.36(-0.40)(+0.46)(stat) +/- 0.06(sys)] x 10(-3) eV(2), $\sin(2)(2)$ (theta) over bar) = 0.86(-0.12)(+0.11)(stat) +/- 0.01(syst). The MINOS $\sin(2)$ nu(mu) and (nu) over bar (mu) measurements are consistent at the 2.0% confidence level, assuming identical underlying oscillation parameters

Physical Review Letters 107[1]. 021801. 2011.

[P123-11] "Generalized Kinetic Equation for Far-from-Equilibrium Many-Body Systems"

Silva, C. A. B., Vasconcellos, A. R., Ramos, J. G., and Luzzi, R.

A kinetic equation for the single particle distribution function in an open many-body system, when in far away from equilibrium conditions is derived in the context of a Non-Equilibrium Thermo-Statistics of ample scope. It consists of a generalization of traditional kinetic equations in that no restrictions are imposed on the characteristics of the nonequilibrium thermodynamic state of the system. This kinetic equation do contain some contributions that become relevant in systems with a nonlinear kinetics when driven sufficiently far from equilibrium (certain complex systems). Moreover, the handling of the kinetic equation in a multiplemoment approach provides a generalized nonlinear higher-order thermo-hydrodynamics

Journal of Statistical Physics 143[5], 1020-1034. 2011.

[P124-11] "Generation of superposition states and chargequbit relaxation probing in a circuit"

Neto, O. P. D., de Oliveira, M. C., and Caldeira, A. O

We demonstrate how a superposition of coherent states can be generated for a microwave field inside a coplanar transmission line coupled to a single superconducting charge qubit, with the addition of a single classical magnetic pulse for chirping of the qubit transition frequency. We show how the qubit dephasing induces decoherence on the field superposition state, and how it can be probed by the qubit charge detection. The character of the charge qubit relaxation process itself is imprinted in the field state decoherence profile

Journal of Physics B-Atomic Molecular and Optical Physics 44[13]. 135503. 2011.

[P125-11] "Higher Harmonic Anisotropic Flow Measurements of Charged Particles in Pb-Pb Collisions at root s(NN)=2.76 TeV"

Aamodt, K., Abelev, B., Quintana, A. A., Adamova, D., Adare, A. M., Aggarwal, M. M., Rinella, G. A., Agocs, A. G., et all

We report on the first measurement of the triangular nu(3), quadrangular nu(4), and pentagonal nu(5) charged particle flow in Pb-Pb collisions at root s(NN) = 2.76 TeV measured with the ALICE detector at the CERN Large Hadron Collider. We show that the triangular flow can be described in terms of the initial spatial anisotropy and its fluctuations, which provides strong constraints on its origin. In the most central events, where the elliptic flow nu(2) and nu(3) have similar magnitude, a double peaked structure in the two-particle azimuthal correlations is observed, which is often interpreted as a Mach cone response to fast partons. We show that this structure can be naturally explained from the measured anisotropic flow Fourier coefficients

Physical Review Letters 107[3]. 032301. 2011.

[P126-11] "Influence of the vibrational modes in the transmission of electronic states of trapped ions in different coupled cavities"

Nohama, F. K. and Roversi, J. A.

In this paper, we present a system formed by two electromagnetic cavities coupled by an optical fibre, each one interacting with a trapped ion. In the carrier band, we observe the one-qubit state transfer between the internal state of the ions and how the transmission time can be influenced by the vibration motion of the ions

Journal of Physics B-Atomic Molecular and Optical Physics 44[11]. 115507. 2011.

[P127-11] "Initial value representation for the SU(n) semiclassical propagator"

Viscondi, T. F. and de Aguiar, M. A. M.

The semiclassical propagator in the representation of SU(n) coherent states is characterized by isolated classical trajectories subjected to boundary conditions in a doubled phase space. In this paper, we recast this expression in terms of an integral over a set of initial-valued trajectories. These trajectories are monitored by a filter that collects only the appropriate contributions to the semiclassical approximation. This framework is suitable for the study of bosonic dynamics in n modes with fixed total number of particles. We exemplify the method for a Bose-Einstein condensate trapped in a triple-well potential, providing a detailed discussion on the accuracy and efficiency of the procedure. (C) 2011 American Institute of Physics. [doi:10.1063/1.3601344]

Journal of Chemical Physics 134[23]. 234105. 2011.

[P128-11] "Mechanical and electrical properties of red blood cells using optical tweezers"

Fontes, A., Castro, M. L. B., Brandao, M. M., Fernandes, H. P., Thomaz, A. A., Huruta, R. R., Pozzo, L. Y., Barbosa, L. C., Costa, F. F., Saad, S. T. O., and Cesar, C. L.

Optical tweezers are a very sensitive tool, based on photon momentum transfer, for individual, cell by cell, manipulation and measurements, which can be applied to obtain important properties of erythrocytes for clinical and research purposes. Mechanical and electrical properties of erythrocytes are critical parameters for stored cells in transfusion centers, immunohematological tests performed in transfusional routines and in blood diseases. In this work, we showed methods, based on optical tweezers, to study red blood cells and applied them to measure apparent overall elasticity, apparent membrane viscosity, zeta potential, thickness of the double layer of electrical

charges and adhesion in red blood cells

Journal of Optics 13[4]. 044012. 2011.

[P129-11] "Model-independent data reductions of elastic proton-proton scattering"

Fagundes, D. A., Menon, M. J., and Silva, G. L. P

New developments in empirical analyses of the proton-proton differential cross section data at high energies are reported. Making use of an unconstrained model-independent parametrization for the scattering amplitude and two different fit procedures, all the experimental data in the center-of-mass energy interval 19.4-62.5 GeV are quite well described (optical point and data above the region of Coulomb-nuclear interference). The contributions from the real and imaginary parts of the amplitude beyond the forward direction are discussed and compared with the results from previous analyses and phenomenological models. Extracted overlap functions (impact parameter space) are outlined and a critical discussion on model-independent analyses and results are also presented

European Physical Journal C 71[5]. 1637. 2011.

[P130-11] "Natural radioactivity and radon exhalation rate in Brazilian igneous rocks"

Moura, C. L., Artura, A. C., Bonotto, D. M., Guedes, S., and Martinelli, C. D.

This paper reports the natural radioactivity of Brazilian igneous rocks that are used as dimension stones, following the trend of other studies on the evaluation of the risks to the human health caused by the rocks radioactivity as a consequence of their use as cover indoors. Gamma-ray spectrometry has been utilized to determine the (40)K, (226)K, and (232)Th activity concentrations in 14 rock types collected at different quarries. The following activity concentration range was found: 12.18-251.90~Bq/kg for (226)Ra, 9.55-347.47 Bq/kg for (232)Th and 407.5-1615.0 Bg/kg for (40)K. Such data were used to estimate Ra(eq) H(ex) and I(gamma), which were compared with the threshold limit values recommended in literature. They have been exceeded for Ra(eq) and H(ex) in five samples, where the highest indices corresponded to a rock that suffered a process of ductile-brittle deformation that caused it a microbrecciated shape. The exhalation rate of Rn and daughters has also been determined in slabs consisting of rock pieces similar to 10 cmlong, 5 cm-wide and 3 cm-thick. It ranged from 0.24 to 3.93 Bq/m(2)/h and exhibited significant correlation with eU (=(226)Ra), as expected. The results indicated that most of the studied rocks did not present risk to human health and may be used indoors, even with low ventilation. On the other hand, igneous rocks that yielded indices above the threshold limit values recommended in literature may be used outdoors without any restriction or indoors with ample ventilation. (C) 2011 Elsevier Ltd. All rights reserved

Applied Radiation and Isotopes 69[7], 1094-1099. 2011.

[P131-11] "Observation of the antimatter helium-4 nucleus"

Agakishiev, H., Aggarwal, M. M., Ahammed, Z., Alakhverdyants, A. V., Alekseev, I., Alford, J., Anderson, B. D., Anson, C. D., Arkhipkin, D., Averichev, G. S., Balewski, J., et all

High-energy nuclear collisions create an energy density similar to that of the Universe microseconds after the Big Bang(1); in both cases, matter and antimatter are formed with comparable abundance. However, the relatively short-lived expansion in nuclear collisions allows antimatter to decouple quickly from matter, and avoid annihilation. Thus, a high-energy accelerator

of heavy nuclei provides an efficient means of producing and studying antimatter. The antimatter helium-4 nucleus ((4)(He) over bar), also known as the anti-alpha ((alpha) over bar), consists of two antiprotons and two antineutrons (baryon number B = -4). It has not been observed previously, although the alphaparticle was identified a century ago by Rutherford and is present in cosmic radiation at the ten per cent level(2). Antimatter nuclei with B -1 have been observed only as rare products of interactions at particle accelerators, where the rate of antinucleus production in high-energy collisions decreases by a factor of about 1,000 with each additional antinucleon(3-5). Here we report the observation of (4)<(He) over bar, the heaviest observed antinucleus to date. In total, 18 (4)(He) over bar counts were detected at the STAR experiment at the Relativistic Heavy Ion Collider (RHIC; ref. 6) in 10(9) recorded gold-on-gold (Au+Au) collisions at centre-of-mass energies of 200 GeV and 62 GeV per nucleon-nucleon pair. The yield is consistent with expectations from thermodynamic(7) and coalescent nucleosynthesis(8) models, providing an indication of the production rate of even heavier antimatter nuclei and a benchmark for possible future observations of (4)(He) over bar in cosmic radiation

Nature 473[7347], 353-356. 2011.

[P132-11] "Optical analogue of the Aharonov-Bohm effect using anisotropic media"

Dartora, C. A., Nobrega, K. Z., and Cabrera, G. G.

We show that in the context of paraxial optics, which can be analyzed through a wave equation similar to the non-relativistic Schrodinger equation of quantum mechanics but replacing time t by spatial coordinate z. the existence of a vector potential A(perpendicular to) mimicking the magnetic vector potential in quantum mechanics is allowed by specific gauge symmetries of the optical field in a medium with anisotropic refractive index. In this way, we use Feynman's path integral to demonstrate an optical analogue of the quantum-mechanical Aharonov-Bohm effect, encouraging the search for another optical systems with analogies with more complex quantum field theories. (C) 2011 Elsevier B.V. All rights reserved

Physics Letters A 375[23], 2254-2257. 2011.

[P133-11] "Optical tweezers for studying taxis in parasites"

de Thomaz, A. A., Fontes, A., Stahl, C. V., Pozzo, L. Y., Ayres, D. C., Almeida, D. B., Farias, P. M. A., Santos, B. S., Santos-Mallet, J., Gomes, S. A. O., Giorgio, S., Feder, D., and Cesar, C. L.

In this work we present a methodology to measure force strengths and directions of living parasites with an optical tweezers setup. These measurements were used to study the parasites chemotaxis in real time. We observed behavior and measured the force of: (i) Leishmania amazonensis in the presence of two glucose gradients; (ii) Trypanosoma cruzi in the vicinity of the digestive system walls, and (iii) Trypanosoma rangeli in the vicinity of salivary glands as a function of distance. Our results clearly show a chemotactic behavior in every case. This methodology can be used to study any type of taxis, such as chemotaxis, osmotaxis, thermotaxis, phototaxis, of any kind of living microorganisms. These studies can help us to understand the microorganism sensory systems and their response function to these gradients

Journal of Optics 13[4]. 044015. 2011.

[P134-11] "Ordered phases of encapsulated diamondoids into carbon nanotubes"

Legoas, S. B., dos Santos, R. P. B., Troche, K. S., Coluci, V. R., and Galvao, D. S. $\,$

Diamondoids are hydrogen-terminated nanosized diamond fragments that are present in petroleum crude oil at low concentrations. These fragments are found as oligomers of the smallest diamondoid, adamantane (C(10)H(16)). Due to their small size, diamondoids can be encapsulated into carbon nanotubes to form linear arrangements. We have investigated the encapsulation of diamondoids into single walled carbon nanotubes with diameters between 1.0 and 2.2 nm using fully atomistic simulations. We performed classical molecular dynamics and energy minimizations calculations to determine the most stable configurations. We observed molecular ordered phases (e. g. double, triple, 4- and 5-stranded helices) for the encapsulation of adamantane, diamantane, and dihydroxy diamantane. Our results also indicate that the functionalization of diamantane with hydroxyl groups can lead to an improvement on the molecular packing factor when compared to nonfunctionalized compounds. Comparisons to hard-sphere models revealed differences, especially when more asymmetrical diamondoids were considered. For larger diamondoids (i.e., adamantane tetramers), we have not observed long-range ordering but only a tendency to form incomplete helical structures. Our calculations predict that thermally stable (at least up to room temperature) complex ordered phases of diamondoids can be formed through encapsulation into carbon nanotubes

Nanotechnology 22[31]. 315708. 2011.

[P135-11] "Pion femtoscopy in p plus p collisions at root s=200 GeV"

Aggarwal, M. M., Ahammed, Z., Alakhverdyants, A. V., Alekseev, I., Alford, J., Anderson, B. D., Arkhipkin, D., Averichev, G. S., Balewski, J., Barnby, L. S., Baumgart, S., et all

The STAR Collaboration at the BNL Relativistic Heavy Ion Collider has measured two-pion correlation functions from p+p collisions at root s = 200 GeV. Spatial scales are extracted via a femtoscopic analysis of the correlations, though this analysis is complicated by the presence of strong nonfemtoscopic effects. Our results are put into the context of the world data set of femtoscopy in hadron-hadron collisions. We present the first direct comparison of femtoscopy in p+p and heavy ion collisions, under identical analysis and detector conditions

Physical Review C 83[6]. 064905. 2011.

[P136-11] "Plasmon polaritons in 1D Cantor-like fractal photonic superlattices containing a left-handed material"

Mejia-Salazar, J. R., Porras-Montenegro, N., Reyes-Gomez, E., Cavalcanti, S. B., and Oliveira, L. E.

The propagation of light incident upon a 1D photonic superlattice consisting of successive stacking of alternate layers of a right-handed nondispersive material and a wmetamaterial, arranged to form a Cantor-like fractal, is considered. Plasmon-polariton excitations are thoroughly investigated within the transfer-matrix approach and shown to strongly depend on the Cantor step number N. More specifically, the number of plasmon-polariton bands corresponds to the number 2(N) - 1 of metamaterial layers within the unit cell. Copyright (C) EPLA, 2011

Epl 95[2]. 24004. 2011.

[P137-11] "Precise measurements of direct CP violation, CPT symmetry, and other parameters in the neutral kaon system"

Abouzaid, E., Arenton, M., Barker, A. R., Barrio, M., Bellantoni, L., Blucher, E., Bock, G. J., Bown, C., Cheu, E., Coleman, R., Corcoran, M. D., Cox, B., Erwin, A. R., Escobar, C. O., et all

We present precise tests of CP and CPT symmetry based on the full data set of K -> pi pi decays collected by the KTeV experiment at Fermi National Accelerator Laboratory during 1996, 1997, and 1999. This data set contains 16 x 10(6) K -> pi(0)pi(0) and 69 x 10(6) K -> pi(+)pi(-) decays. We measure the direct CP violation parameter Re(epsilon'/epsilon) = (19.2 +/- 2.1) x 10(-4). We find the $K(L) \rightarrow K(S)$ mass difference Delta m = (5270 +/ - 12) x 10(6) (h) over tilde s(-1) and the K(S) lifetime tau(S) = $(89.62 + / - 0.05) \times 10(-12)$ s. We also measure several parameters that test CPT invariance. We find the difference between the phase of the indirect CP violation parameter epsilon and the superweak phase: phi(epsilon) - phi(SW) = (0.40 + / - 0.56)degrees. We measure the difference of the relative phases between the CP violating and CP conserving decay amplitudes for K -> pi(+)pi(-) (phi(+-)) and for K -> pi(0)pi(0) (phi(00)): Delta phi = (0.30 + / 1)0.35)degrees. From these phase measurements, we place a limit on the mass difference between K(0) and (K) over bar (0): Delta M < $4.8 \times 10(-19)$ GeV/c(2) at 95% C.L. These results are consistent with those of other experiments, our own earlier measurements, and CPT symmetry

Physical Review D 83[9]. 092001. 2011.

[P138-11] "Pressure and chemical substitution effects in the local atomic structure of BaFe(2)As(2)"

Granado, E., Mendonca-Ferreira, L., Garcia, F., Azevedo, G. D., Fabbris, G., Bittar, E. M., Adriano, C., Garitezi, T. M., Rosa, P. F. S., Bufaical, L. F., Avila, M. A., Terashita, H., and Pagliuso, P. G.

The effects of K and Co substitutions and quasihydrostatic applied pressure (P < 9 GPa) in the local atomic structure of BaFe(2)As(2), Ba(Fe(0.937)Co(0.063))(2)As(2) and Ba(0.85)K(0.15)Fe(2)As(2) superconductors were investigated by extended x-ray absorption fine structure (EXAFS) measurements in the As K absorption edge. The As-Fe bond length is found to be slightly reduced (less than or similar to 0.01 angstrom) by both Co and K substitutions, without any observable increment in the corresponding Debye-Waller factor. Also, this bond is shown to be compressible [kappa = $3.3(3) \times 10(-3)$ GPa(-1)]. The observed contractions of As-Fe bond under pressure and chemical substitutions are likely related with a reduction of the local Fe magnetic moments, and should be an important tuning parameter in the phase diagrams of the Fe-based superconductors

Physical Review B 83[18]. 184508. 2011.

[P139-11] "Probing the interdependence between irreversible magnetization reversal processes by first-order reversal curves"

Beron, F., Pirota, K. R., and Knobel, M.

A procedure to probe the interdependence between irreversible magnetic processes is presented. It consists of measuring the first-order reversal curves (FORCs) without saturating the system. Depending on the variation of the reversal fields during the curves' acquirement (increasing or decreasing), it fixes the hardest or softest hysterons into their negative saturation level throughout the measurement. Differences between these FORC diagrams and the classical one, as well as variation of the end magnetization as a function of the reversal field, indicate and characterize the requirement that some irreversible processes arise from others. The procedure is described to investigate magnetic systems, but

can be directly used to study any hysteretic system. (C) 2011 American Institute of Physics. [doi:10.1063/1.3538940]

Journal of Applied Physics 109[7]. 07E308. 2011.

[P140-11] "Production of pions, kaons and protons in pp collisions at root s=900 GeV with ALICE at the LHC"

Aamodt, K., Abel, N., Abeysekara, U., Quintana, A. A., Abramyan, A., Adamova, D., Aggarwal, M. M., Rinella, G. A., Agocs, A. G., Salazar, S. A., Ahammed, Z., Ahmad, A., Ahmad, N., et all

The production of pi(+), pi(-), K(+), K(-), p, and (p) over bar at mid-rapidity has been measured in proton-proton collisions at root s = 900 GeV with the ALICE detector. Particle identification is performed using the specific energy loss in the inner tracking silicon detector and the time projection chamber. In addition, time-of-flight information is used to identify hadrons at higher momenta. Finally, the distinctive kink topology of the weak decay of charged kaons is used for an alternative measurement of the kaon transverse momentum (p(t)) spectra. Since these various particle identification tools give the best separation capabilities over different momentum ranges, the results are combined to extract spectra from p(t) = 100 MeV/c to 2.5 GeV/c. The measured spectra are further compared with QCD-inspired models which yield a poor description. The total yields and the mean pt are compared with previous measurements, and the trends as a function of collision energy are discussed

European Physical Journal C 71[6]. 1655. 2011.

[P141-11] "Quantum Critical Kondo Quasiparticles Probed by ESR in beta-YbAlB(4)"

Holanda, L. M., Vargas, J. M., Iwamoto, W., Rettori, C., Nakatsuji, S., Kuga, K., Fisk, Z., Oseroff, S. B., and Pagliuso, P. G.

Electron spin resonance (ESR) can probe conduction Electron spin resonance (ESR) can probe conduction electrons (CE) and local moment (LM) spin systems in different materials. A CE spin resonance (CESR) is observed in metallic systems based on light elements or with enhanced Pauli susceptibility. LM ESR can be seen in compounds with paramagnetic ions and localized d or f electrons. Here we report a remarkable and unprecedented ESR signal in the heavy-fermion superconductor beta-YbAlB(4) [S. Nakatsuji et al., Nature Phys. 4, 603 (2008)] which behaves as a CESR at high temperatures and acquires characteristics of the Yb(3+) LM ESR at low temperature. This dual behavior strikes as an in situ unique observation of the Kondo quasiparticles in a quantum critical regime. The proximity to a quantum critical point may favor the appearance of this dual character of the ESR signal in beta-YbAlB(4)

Physical Review Letters 107[2]. 026402. 2011.

[P142-11] "Reproducing neutrino effects on the matter power spectrum through a degenerate Fermi gas approach"

Perico, E. L. D. and Bernardini, A. E.

Modifications on the predictions about the matter power spectrum based on the hypothesis of a tiny contribution from a degenerate Fermi gas (DFG) test-fluid to some dominant cosmological scenario are investigated. Reporting about the systematic way of accounting for all the cosmological perturbations, through the Boltzmann equation we obtain the analytical results for density fluctuation, delta, and fluid velocity divergence, theta, of the DFG. Small contributions to the

matter power spectrum are analytically obtained for the radiation-dominated background, through an ultra-relativistic approximation, and for the matter-dominated and A-dominated eras, through a non-relativistic approximation. The results can be numerically reproduced and compared with those of considering non-relativistic and ultra-relativistic neutrinos into the computation of the matter power spectrum. Lessons concerning the formation of large scale structures of a DFG are depicted, and consequent deviations from standard ACDM predictions for the matter power spectrum (with and without neutrinos) are quantified

Journal of Cosmology and Astroparticle Physics [6]. 001. 2011.

[P143-11] "Semiclassical propagator for SU(n) coherent states"

Viscondi, T. F. and de Aguiar, M. A. M.

We present a detailed derivation of the semiclassical propagator in the SU(n) coherent state representation. In order to provide support for immediate physical applications, we restrict this work to the fully symmetric irreducible representations, which are suitable for the treatment of bosonic dynamics in n modes, considering systems with conservation of total particle number. The derivation described here can be easily extended to other classes of coherent states, thus representing an alternative approach to previously published methods. (C) 2011 American Institute of Physics. [doi:10.1063/1.3583996]

Journal of Mathematical Physics 52[5]. 052104. 2011.

[P144-11] "Sketched oxide single-electron transistor"

Cheng, G. L., Siles, P. F., Bi, F., Cen, C., Bogorin, D. F., Bark, C. W., Folkman, C. M., Park, J. W., Eom, C. B., Medeiros-Ribeiro, G., and Levy, J.

Devices that confine and process single electrons represent an important scaling limit of electronics(1,2). Such devices have been realized in a variety of materials and exhibit remarkable electronic, optical and spintronic properties(3-5). Here, we use an atomic force microscope tip to reversibly 'sketch' singleelectron transistors by controlling a metal-insulator transition at the interface of two oxides(6-8). In these devices, single electrons tunnel resonantly between source and drain electrodes through a conducting oxide island with a diameter of similar to 1.5 nm. We demonstrate control over the number of electrons on the island using bottom-and side-gate electrodes, and observe hysteresis in electron occupation that is attributed to ferroelectricity within the oxide heterostructure. These singleelectron devices may find use as ultradense non-volatile memories, nanoscale hybrid piezoelectric and charge sensors, as well as building blocks in quantum information processing and simulation platforms

Nature Nanotechnology 6[6], 343-347. 2011.

[P145-11] "Solar neutrino spectrum, sterile neutrinos, and additional radiation in the Universe" de Holanda, P. C. and Smirnov, A. Y.

Recent results from the SNO, Super-Kamiokande, and Borexino experiments do not show the expected upturn of the energy spectrum of events (the ratio R equivalent to N(obs)/N(SSM)) at low energies. At the same time, cosmological observations testify for the possible existence of additional relativistic degrees of freedom in the early Universe: Delta N(eff) 1-2. These facts strengthen the case of a very light sterile neutrino, v(s), with Delta m(01)(2) similar to (0.7-2) X 10(-5) eV(2), which mixes

weakly with the active neutrinos. The v(s) mixing in the mass eigenstate v(1) characterized by $\sin(2)2$ alpha similar to 10(-3) can explain an absence of the upturn. The mixing of v(s) in the eigenstate v(3) with $\sin(2)$ beta similar to 0.1 leads to production of v(s) via oscillations in the Universe and to additional contribution Delta N(eff) approximate to 0.7-1 before the big bang nucleosynthesis and later. Such a mixing can be tested in forthcoming experiments with the atmospheric neutrinos, as well as in future accelerator long baseline experiments. It has substantial impact on conversion of the supernova neutrinos

Physical Review D 83[11]. 113011. 2011.

[P146-11] "Strange particle production in proton-proton collisions at root s=0.9 TeV with ALICE at the LHC"

Aamodt, K., Quintana, A. A., Adamova, D., Adare, A. M., Aggarwal, M. M., Rinella, G. A., Agocs, A. G., Salazar, S. A., Ahammed, Z., Ahmad, N., Masoodi, A. A., Ahn, S. U., et all

The production of mesons containing strange quarks (K(S)(0),phi) and both singly and doubly strange baryons (Lambda, (Lambda) over bar, and Xi(-) + (Xi) over bar (+)) are measured at mid-rapidity in pp collisions at root s = 0.9 TeV with the ALICE experiment at the LHC. The results are obtained from the analysis of about 250 k minimum bias events recorded in 2009. Measurements of yields (dN/dy) and transverse momentum spectra at mid-rapidity for inelastic pp collisions are presented. For mesons, we report yields (< dN/dy >) of 0.184 + - 0.002(stat.) + - 0.006(syst.) for K(S)(0) and 0.021 +/-0.004(stat.) +/-0.003(syst.) for phi. For baryons, we find < dN/dy > = 0.048 +/- 0.001(stat.) +/- 0.004(syst.) for Lambda, 0.047 +/- 0.002(stat.) +/- 0.005(syst.) for (Lambda) over bar and 0.0101 + - 0.0020(stat.) + - 0.0009(syst.) for Xi(-) + (Xi) over bar (+). The results are also compared with predictions for identified particle spectra from QCD-inspired models and provide a baseline for comparisons with both future pp measurements at higher energies and heavy-ion collisions

European Physical Journal C 71[3]. 1594. 2011.

[P147-11] "The invariance of the total direct DNA strand break yield"

Bernal, M. A., deAlmeida, C. E., Sampaio, C., Incerti, S., Champion, C., and Nieminen, P.

Purpose: The invariance of the total direct strand break yield when DNA is irradiated by different types of particles and energies has been reported by previous works. This study is intended to explain the physical causes of this behavior. Methods: The GEANT4-DNA extension of the GEANT4 general purpose Monte Carlo simulation toolkit has been used to determine direct strand break yields induced by protons and alpha particles impacting on a B-DNA geometrical model, including five organization levels of the human genetic material. The linear energy transfer (LET) of such particles ranges from 4.8 keV/ mu m (10 MeV protons) to about 235 keV/mu m (2 MeV alpha particles), at 5.225 mu m depth (near the center of the region of interest). Direct total, single and double strand break probabilities have been determined in a liquid water homogeneous medium with a 1.06 g/cm (3) density. The energetic spectra of single strand breaks (SSB), the number of energy deposition events, and the SSB/event ratio were determined. Results: The target-hit probability was found to be independent of both the type and the energy of the incident particle, even if this latter is a secondary electron. This probability is determined by the geometrical properties of the system. The total strand break yield and the number of energy deposition events required to reach a certain absorbed dose were found nearly independent of the type and energy of the incident ion (proton or alpha). In contrast, the double strand

break (DSB) yield was found strongly dependent on the LET of the incident radiation. Conclusions: The SSB generation process is homogeneous and independent of the LET of the particles involved, at least within the proton and alpha particle energy range here studied. The target-hit probability is only determined by the ratio between the total volume occupied by targets and that of the ROI where the radiation deposits its energy. The maximum separation distance between two adjacent SSBs to produce a DSB is the parameter that breaks the homogeneity of the target-hit process, making the DSB production process strongly heterogeneous. (C) 2011 American Association of Physicists in Medicine. [DOI: 10.1118/1.3597568]

Medical Physics 38[7], 4147-4153. 2011.

[P148-11] "The Pierre Auger Observatory scaler mode for the study of solar activity modulation of galactic cosmic rays"

Abreu, P., Aglietta, M., Ahn, E. J., Allard, D., Allekotte, I., Allen, J., Castillo, J. A., Alvarez-Muniz, J., Ambrosio, M., Aminaei, A., Anchordoqui, L., Andringa, S., Anticic, T., Anzalone, A., et all

Since data-taking began in January 2004, the Pierre Auger Observatory has been recording the count rates of low energy secondary cosmic ray particles for the self-calibration of the ground detectors of its surface detector array. After correcting for atmospheric effects, modulations of galactic cosmic rays due to solar activity and transient events are observed. Temporal variations related with the activity of the heliosphere can be determined with high accuracy due to the high total count rates. In this study, the available data are presented together with an analysis focused on the observation of Forbush decreases, where a strong correlation with neutron monitor data is found

Journal of Instrumentation 6. P01003. 2011.

[P149-11] "Third edge for a graphene nanoribbon: A tight-binding model calculation"

Bahamon, D. A., Pereira, A. L. C., and Schulz, P. A.

The electronic and transport properties of an extended linear defect embedded in a zigzag nanoribbon of realistic width are studied within a tight-binding model approach. Our results suggest that such a defect profoundly modifies the properties of the nanoribbon, introducing new conductance quantization values and modifying the conductance quantization thresholds. The linear defect along the nanoribbon behaves as an effective third edge of the system, which shows a metallic behavior, giving rise to new conduction pathways that could be used in nanoscale circuitry as a quantum wire

Physical Review B 83[15]. 155436. 2011.

[P150-11] "van der Waals potential barrier for cobaltocene encapsulation into single-walled carbon nanotubes: classical molecular dynamics and ab initio study"

Azevedo, D. L., Sato, F., de Sousa, A. G., and Galvao, D. S.

In this work, we carried out geometry optimisations and classical molecular dynamics for the problem of cobaltocene (CC) encapsulation into different carbon nanotubes (CNTs) ((7,7), (8,8), (13,0) and (14,0) tubes were used). CCs are molecules composed of two aromatic pentagonal rings (C5H5) sandwiching one cobalt atom. From our simulation results, we observed that CC was encapsulated into CNTs (8,8), (13,0) and (14,0). However, for CNT (7,7), the encapsulation could not occur, in disaggrement with some previous works in the literature. Our results show that the encapsulation process is mainly governed by van der

Waals potential barriers

Molecular Simulation 37[9], 746-751. 2011.

Material Editorial

"Vannevar Bush: an introduction"

Cruz, C. H. B.

Revista Latinoamericana de Psicopatologia Fundamental 14[1], 11-13. 2011.

Capítulo de Livro

Vênus, brincadeira de roda e o fim do geocentrismo. Paixão, F. J. In: Pavão, A.C. (coord.) **Ciências:** ensino fundamental. Brasília: Ministério da Educação, 2010. Cap.6, p.89-100. (Coleção Explorando o Ensino)

Nota: Disponível no portal do MEC.

Errata: Os autores do artigo PO89 são:

[P089-11] "Search for first harmonic modulation in the right ascension distribution of cosmic rays detected at the Pierre Auger Observatory"

Abreu, P., Aglietta, M., Ahn, E. J., Albuquerque, I. F. M., Allard, D., Allekotte, I., Allen, J., Allison, P., Castillo, J. A., Alvarez-Muniz, J., Ambrosio, M., Aminaei, A., Anchordoqui, L., Andringa, S., Anticic, T., Aramo, C., Arganda, E., et all

We present the results of searches for dipolar-type anisotropies in different energy ranges above 2.5 x 10(17) eV with the surface detector array of the Pierre Auger Observatory, reporting on both the phase and the amplitude measurements of the first harmonic modulation in the right-ascension distribution. Upper limits on the amplitudes are obtained, which provide the most stringent bounds at present, being below 2% at 99% C.L. for EeV energies. We also compare our results to those of previous experiments as well as with some theoretical expectations. (C) 2011 Elsevier B.V. All rights reserved

Astroparticle Physics 34[8], 627-639. 2011.

Abstracta

Instituto de Física

Diretor: Prof. Dr. Daniel Pereira

Universidade Estadual de Campinas - UNICAMP

Cidade Universitária Zeferino Vaz 13083-859 - Campinas - SP - Brasil

e-mail: secdir@ifi.unicamp.br Fone: 0XX 19 3521-5300

Publicação

Biblioteca do Instituto de Física Gleb Wataghin http://webbif.ifi.unicamp.br Diretora Técnica: Sandra Maria Carlos Cartaxo

Elaboração Antonela Carvalho Ribeiro antonela@ifi.unicamp.br

Projeto Gráfico ÍgneaDesign

Impressão

Gráfica Central - Unicamp